# Fullerene Quantum Gyroscope

M. Krause,[1,2] M. Hulman,[1,*] H. Kuzmany,[1] O. Dubay,[1] G. Kresse,[1] K. Vietze,[3] G. Seifert,[3] C. Wang,[4] and H. Shinohara[4]

[1]*Institut für Materialphysik der Universität Wien, Wien, Austria*

[2]*Institut für Festkörper- and Werkstofforschung, Dresden, Germany*

[3]*Institut für Physikalische Chemie, Technische Universität Dresden, Germany*

[4]*Department of Chemistry and Institute for Advanced Research, Nagoya University, Nagoya, Japan*

(Received 12 February 2004; published 22 September 2004)

We report the observation of quantized rotational states of a diatomic $C_2$ unit in solid endohedral fullerene $C_2Sc_2@C_{84}$. The rotational transitions induce a periodic line pattern in the low energy Raman spectrum. The rotational constant $B$ and the C-C distance were found to be 1.73 $cm^{-1}$ and 0.127 nm, respectively. Density functional calculations revealed an intrinsic rotational barrier of the order of only a few meV for the $C_2$ unit. The Schrödinger equation involving the potential barrier was solved and the Raman tensor matrix elements were calculated, yielding good quantitative agreement with the experiment. To our best knowledge this is the first intrinsic rotational spectrum of a diatomic plane molecular rotor.

DOI: 10.1103/PhysRevLett.93.137403 PACS numbers: 78.30.Na, 33.15.Dj, 33.15.Hp, 33.15.Mt

The tight shielding provided by carbon cages allows one to grow new and unique materials inside these curved nanospaces. In the case of higher fullerenes, molecular clusters could be encapsulated which do not exist outside the cages. Outstanding examples are the trimetallnitride cluster molecules of the general formulae $M_3N$, where $M$ is Sc, Y, or a rare earth element encaged in $C_{80}$ [1,2]. Another species is $Sc_2C_2$ in $C_{84}$ [3]. The rather weak interaction between the endohedral cluster and the carbon cage allows for an interesting dynamics of the encaged species. In agreement with theoretical predictions [4], so far the nature of this dynamics was always a diffuse motion.

In this Letter we demonstrate the existence of quantized rotational states of the $C_2$ unit in the form of a rigid rotor in crystalline $C_2Sc_2@C_{84}$. The related transitions were identified in the low energy Raman spectra and were observable up to an unusual high temperature of 200 K. According to x-ray powder diffraction data, the two scandium ions are accommodated on the $C_2^{(z)}$ ($S_4^{(z)}$) axis of the $D_{2d}$-$C_{84}$ cage. The $C_2$ group is located at the cage center with orientation perpendicular to $C_2^{(z)}$ [3].

Drop coated thin films of $C_2Sc_2@C_{84}$ were prepared on gold covered Si substrates from toluene solution and subsequently annealed in high vacuum at 500 K for several hours. Raman experiments were carried out in the backscattering geometry for temperatures between 25 and 300 K for red (647 nm) and green (514 nm) laser excitation with 1.5 $cm^{-1}$ resolution. Line positions and widths were determined by fitting Voigtian profiles after subtraction of the elastic stray-light background.

Density functional tight binding (DFTB) and *ab initio* density functional (DFT) calculations were carried out to obtain reliable information on the structure and electronic properties of the system. The former calculations were supplemented by a molecular-dynamical (MD) analysis. For the DFT calculations the Vienna *ab initio* simulation package (VASP) was used [5,6].

Figure 1 presents the molecular structure obtained from molecular dynamics calculations. These calculations provide a first indication that $C_2@Sc_2C_{84}$ is a more realistic formula than $C_2Sc_2@C_{84}$ for the material under study. The DFT calculations revealed 0.444, 0.128, and 0.224 nm for the Sc-Sc, C-C, and Sc-cage distances, respectively, in very good agreement with the results obtained by Wang *et al.* A total charge of $-2e$, $+3e$, and $-4e$ is predicted for the $C_2$ group, each Sc ion, and the cage, respectively, using both theoretical methods.

Figure 2 shows the Raman spectra of $C_2@Sc_2C_{84}$ in the low frequency spectral region between 10 and 150 $cm^{-1}$. The observed frequency patterns for the two excitations are almost identical. Two rather strong and partly structured lines at 100 and 126 $cm^{-1}$ can be assigned to a Sc-$C_{84}$ mode and a translational motion of the $C_2$ molecule as a result of the present calculations. On the low

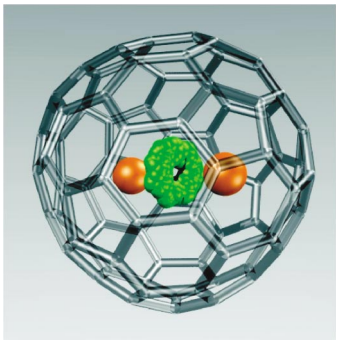

FIG. 1 (color online). Structure of $C_2@Sc_2C_{84}$. The two spheres represent the Sc ions on the $C_2(z)$ symmetry axis; the $y$ axis lies in plane of the sheet. The central part of the figure represents a superposition of carbon states as evaluated from DFTB MD calculations at 300 K.

  

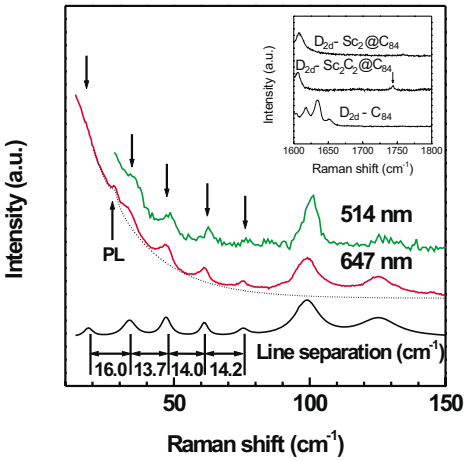


FIG. 2 (color online). Low energy Raman spectra for $C_2@Sc_2C_{84}$ at 80 K. The dotted line is an exponential background and the full line is the fit using Voigtian lines. PL identifies a plasma line. The arrows indicate positions for equidistant Raman lines. The inset shows the high-energy part of the spectra for $Sc_2C_{84}$, $C_2@Sc_2C_{84}$, $C_{84}$ (from top to bottom). The arrow points to the C-C vibration at 1745 $cm^{-1}$ which is missing in $C_{84}$ and $C_2@C_{84}$.

energy side of these modes we observe five almost equidistant lines. Such line patterns have not been observed in Raman spectra of fullerenes so far. The equidistant character of these lines suggests to assign them to quantized rotational states of the $C_2$ unit. The inset of Fig. 2 shows a single line at 1745 $cm^{-1}$ which is present neither in $C_{84}$ nor in $Sc_2@C_{84}$. Thus, this line was assigned to the stretch vibration of the $C_2$ molecule inside the fullerene cage in excellent agreement with a value of 1742 $cm^{-1}$ found from our *ab initio* DFT calculations.

The line pattern of rotational Raman spectra are well known for gases [7]. In the solid state, resolved rotational spectra are really rare. The classical example is crystalline hydrogen, whose rotational Raman spectrum at temperatures below the melting point of 13 K reveals two-dimensional quasi-undistorted hydrogen rotation [8]. Quasi-2D states of a plane rotor were found for $H_2$ in intercalated graphite [9], on a stepped copper surface [10], and for interstitial atomic oxygen in germanium [11]. Rotational lines of $C_2$ were only observed in the gas phase as structures accompanying electronic transitions in hot carbon plasma [12–14].

For the unperturbed diatomic rotor, rotations occur around an axis free in space with energy eigenvalues $E(J) = BJ(J+1) = \{[J(J+1)h]/(8\pi^2 c_0 I_M)\}$, where $I_M$ is the momentum of inertia, $B$ the rotational constant (in $cm^{-1}$), and $J$ the angular momentum quantum number. If rotations are restricted to a plane the eigenenergies are $E(m) = Bm^2$, $m = 0, \pm 1, \pm 2, \ldots$. Since the carbon nucleus has zero spin it is of bosonic type and requires totally symmetric wave function with respect to the permutation of the two nuclei. Within the Born-Openheimer approximation the wave function of a molecule is given by $\psi = \psi_e \psi_v \psi_r \psi_{ns}$ where $\psi_e$ represents the electronic, $\psi_v$ the vibrational, $\psi_r$ the rotational, and $\psi_{ns}$ the nuclear spin wave function. Since the nuclear spin is zero for $^{12}C$, $\psi_{ns}$ is symmetric. The same holds for $\psi_v$ as we are studying pure rotational transitions without vibronic contributions. Furthermore, the electron wave function of the $C_2^{2-}$ unit is totally symmetric (closed-shell configuration). In this case only even rotational states are allowed. The selection rule for Raman scattering of a free and plane rotating diatomic molecule is $\Delta J = \pm 2$ and $\Delta m = \pm 2$, respectively. Hence a line separation of $8B$ is expected for both cases. The position of the first line is, however, different for the free rotor (at $6B$) and its plane counterpart (at $4B$). From the observed average distance of 13.8 $cm^{-1}$ between the rotational lines the rotational constant $B$ turns out to be 1.73 $cm^{-1}$ and the resulting moment of inertia reveals the value $1.617 \times 10^{-46}$ kg $m^2$. This gives 0.127 nm for the C-C distance of the rotor in excellent agreement with the length obtained from the stretching frequency and from the DFT calculations (0.128 nm).

Results for the line positions are listed in the left part of Table I for the unperturbed plane and free rotors. It is evident that the experimental values follow closely those for the plane rotor at least for the higher transitions. In the low energy range more lines were observed than expected from the calculations for the unperturbed plane rotor.

In order to check the intensity profiles of rotational spectra we investigated the low energy Raman scattering of $C_2@Sc_2C_{84}$ as a function of temperature in the range between 25 and 200 K. Selected spectra are depicted in Fig. 3. At low temperatures, up to about 60 K, the lowest energy members of the equidistant line set dominate the spectrum. At higher temperatures Raman peaks corresponding to higher quantum numbers, such as the peaks at 49 or 63 $cm^{-1}$, gain in intensity and the first peak in the series is completely lost. From about 120 K on, the lines start to broaden dramatically, until at temperatures of 200 K and above they become very broad and eventually disappear from the spectrum. In contrast, the lines at 100 $cm^{-1}$ and above remain observable with a moderate broadening and a small temperature induced shift.

For a given temperature the intensity for the plane rotor is $I(m, T) = 2e^{-E(m)/k_B T} (m \neq 0)$. This means the intensities are continuously decreasing with increasing energy. However, the experimental results for higher temperatures (line pattern at the bottom of Figs. 2 and 3) are not consistent with this behavior.

An unperturbed rotational state can only be anticipated if the rotational barriers are zero or at least very small. This is not trivial in our case, since there is considerable Coulomb interaction and even some covalent overlap between the dicarbon molecule and the Sc ions. From *ab initio* DFT calculations a rotational barrier of the order of 4 meV (at 0 K) around the $z$ axis was found, whereas the barrier for rotation around $x$ is of the order of eV. The inset

TABLE I. (Left part) Comparison of the experiment with as calculated positions of the rotational lines for the unperturbed plane and free rotors. Raman transitions are assigned for the plane rotor. (Right part) The same for the perturbed plane rotor. The assignment of the Raman transitions is also given. The experimental values were taken from the spectrum at 40 K, $B = 1.73\ \mathrm{cm}^{-1}$, and $q = -2$. For $\pm$ signs see Fig. 4. A plasma line is at $29.6\ \mathrm{cm}^{-1}$.

| Experiment ($\mathrm{cm}^{-1}$) | Unperturbed plane rotor (calc., $\mathrm{cm}^{-1}$) | Unperturbed free rotor (calc., $\mathrm{cm}^{-1}$) | Perturbed plane rotor (calc., $\mathrm{cm}^{-1}$) | |
|---|---|---|---|---|
| | | | 4.1 | $0 \rightarrow 2+$ |
| 11.0 | | | 11.0 | $0 \rightarrow 2-$ |
| 18.5 | 20.8 ($2 \rightarrow 4$) | 24.2 | 17.4 | $2- \rightarrow 4-$ |
| | | | 18.2 | $2- \rightarrow 4+$ |
| 25.0 | | | 24.3 | $2+ \rightarrow 4-$ |
| | | | 25.1 | $2+ \rightarrow 4+$ |
| 34.7 | 34.6 ($4 \rightarrow 6$) | 38.1 | 34.0 | $4+ \rightarrow 6\pm$ |
| | | | 34.0 | $4- \rightarrow 6\pm$ |
| 48.6 | 48.4 ($6 \rightarrow 8$) | 51.9 | 48.4 | $6\pm \rightarrow 8\pm$ |
| 62.2 | 62.3 ($8 \rightarrow 10$) | 65.7 | 62.3 | $8\pm \rightarrow 10\pm$ |
| 76.0 | 76.1 ($10 \rightarrow 12$) | 79.6 | 76.1 | $10\pm \rightarrow 12\pm$ |

of Fig. 4 depicts the potential energy the rotor encounters on its circular motion around $z$. The potential has a fourfold symmetry and can be well approximated by a cosine function.

We solved the Schrödinger equation for a plane rotor $[-B(\partial^2/\partial\gamma^2) - E + V(\gamma)]\phi = 0$ with the potential term $V(\gamma) = V_0(1 - \cos 4\gamma)/2$. Substituting for $q = -V_0/4B$ and $a = E/B + 2q$ we obtain the well known Mathieu's equation [15]. Its eigenenergies are shown in Fig. 4 for a wide range of rotational barrier heights. It is evident that the eigenenergies of the higher rotational level are not affected significantly by the potential and the levels remain unsplit. On the other hand, splitting of the rotational levels leads to the multicomponent nature of the spectra at low energies.

In order to assign the positions of the rotational lines as well as to explain the peculiar behavior of the Raman intensities we calculated Raman tensor matrix elements. Assuming the incident light propagates along the positive $z$ axis and is polarized in the $y$ direction in the laboratory fixed coordinate system, two different polarizations contribute to the intensity of the backscattered light. The total intensity $I$ is obtained by averaging the two contributions $I \sim |\langle\phi_f|\alpha_{yy}|\phi_i\rangle|^2 + |\langle\phi_f|\alpha_{xy}|\phi_i\rangle|^2$ over all orientations of the $C_2$ molecules, where $\phi_i$ and $\phi_f$ are the rotational wave functions of the initial and final states, respectively. $\alpha_{yy}$ and $\alpha_{xy}$ are the Cartesian components of the Raman tensor. We define a coordinate system rotating with the $C_2$ molecule, such that the Raman tensor is diagonal with the Cartesian components $(\alpha_\perp, \alpha_\perp, \alpha_\parallel)$.

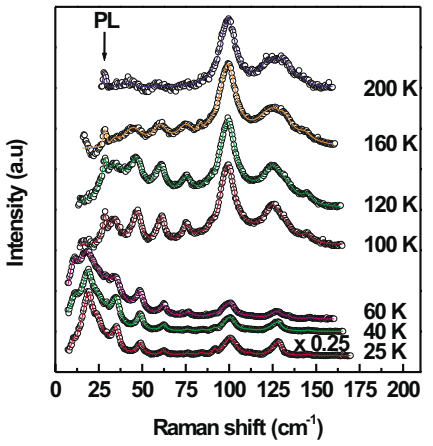


FIG. 3 (color online). Low energy Raman response of $C_2@Sc_2C_{84}$ as recorded with the red laser for selected temperatures indicated and after background subtraction.

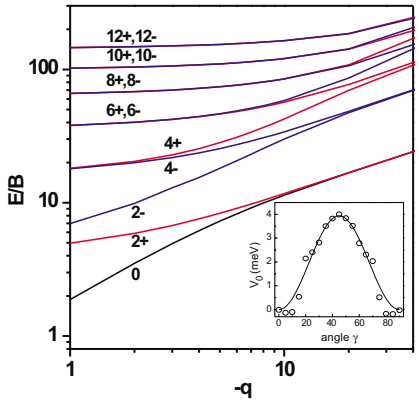


FIG. 4 (color online). Eigenenergies of the perturbed plane rotor as a function of the dimensionless parameter, $q = -V_0/4B$. Only those energies are displayed which belong to the unperturbed rotational states with even $m$. Numbers denote the values of the quantum state $m$ in the absence of the potential; $\pm$ signs refer to the parity of the wave function upon inversion, $\gamma \rightarrow -\gamma$. The inset shows the rotational potential obtained from *ab initio* calculations (circles) and the fit with the function $V(\gamma) = V_0(1 - \cos 4\gamma)/2$ (solid line).

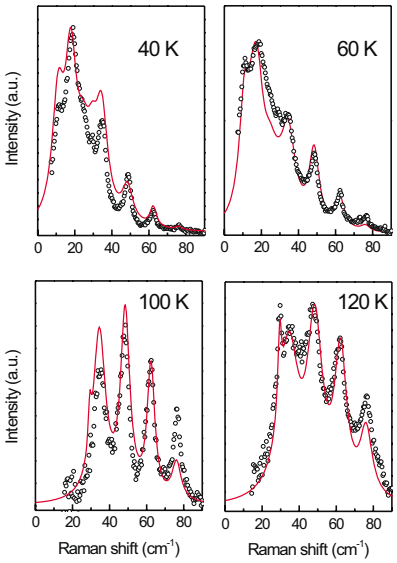


FIG. 5 (color online). Experimental (circles) and as calculated (solid lines) rotational spectra of the $C_2$ molecule for different temperatures. Linewidths of the as calculated lines were taken from the experiment. The intensity was normalized to the maximum intensity of the experimental spectrum.

Following the standard procedure [16], the Cartesian components $\alpha_{xy}$ and $\alpha_{yy}$ can be expressed as a function of the Euler angles $(\alpha, \beta, \gamma)$:

$$\alpha_{yy}(\beta, \gamma) = -\frac{a}{3} - \frac{b}{6}[3\cos^2(\beta) - 1] - \frac{b}{2}\sin^2(\beta)\cos(2\gamma),$$

$$\alpha_{xy}(\beta, \gamma) = -\frac{b}{2}\sin^2(\beta)\sin(2\gamma), \quad (1)$$

where $a = 2\alpha_\perp + \alpha_\parallel$ and $b = \alpha_\parallel - \alpha_\perp$. After integration over $\beta$ of an ensemble of randomly oriented molecules one obtains for the Raman scattering intensities $(\phi_f \neq \phi_i)$:

$$|\langle\phi_f|\alpha_{yy}|\phi_i\rangle|^2 = \frac{4}{15}b^2\left|\int_0^{2\pi}\phi_f(\gamma)\cos(2\gamma)\phi_i(\gamma)d\gamma\right|^2, \quad (2)$$

$$|\langle\phi_f|\alpha_{xy}|\phi_i\rangle|^2 = \frac{4}{15}b^2\left|\int_0^{2\pi}\phi_f(\gamma)\sin(2\gamma)\phi_i(\gamma)d\gamma\right|^2. \quad (3)$$

The selection rule $\Delta m = \pm 2$ for the plane rotor follows immediately from the above equations.

The only adjustable parameter defining the energy scale is $q$, the ratio between the potential barrier and the rotational constant. Positions of the rotational lines are listed in the right part of Table I for $q = -2$ and compared with the experimental values at 40 K. The agreement is excellent.

The corresponding barrier height is 1.7 meV which is roughly one-half of the value obtained from *ab initio* calculations. The discrepancy is small relative to the absolute binding energy of the $C_2$ in the $Sc_2C_{84}$ cage (several eV), and it can easily originate from inaccuracies of the semilocal density functionals as well as to the neglect of any coupling to vibrational modes.

The Raman line intensities were calculated by multiplying the matrix elements from Eqs. (2) and (3) by the Boltzmann factor $e^{-E/k_BT}$, where $E$ is the energy of the initial state. The linewidths were taken from the experiment and were allowed to vary in $\pm 30\%$ with respect to the experimental values. The results are shown in Fig. 5 for several temperatures. The overall agreement is again very good. Only the intensities of the highest rotational line are underestimated. In contrast to the unperturbed rotor the intensity profiles are not merely determined by the Boltzmann factor. Whereas at low temperatures the factor strongly suppresses the intensity of the higher rotational lines, at moderate temperatures the matrix elements start to play a decisive role.

To conclude, we have observed a planar $C_2$ rotor in a solid consisting of $Sc_2C_{84}$ molecules, a quantum gyroscope with a cardanic suspension. The system provides the first experimental realization of a diatomic plane molecular rotor, a 70-year-old textbook example of quantum mechanics [17].

This work was supported by the EU Project NANOTEMP (HPRN-CT-2002-00192), the Austrian FWF (14995-PHY), and by the EU, TMR Project FULPROP.

*Corresponding author.
Email address: hulman@ap.univie.ac.at

[1] S. Stevenson *et al.*, Nature (London) **401**, 55 (1999).
[2] M. Krause *et al.*, J. Chem. Phys. **111**, 7976 (1999).
[3] C. Wang *et al.*, Angew. Chem. **113**, 411 (2001).
[4] W. Andreoni and A. Curioni, Appl. Phys. A **66**, 299 (1998).
[5] VASP [6] was used in the PBE generalized gradient approximation, the projector augmented wave method and a plane wave cutoff of 400 eV.
[6] G. Kresse, and J. Furthmüller, Comput. Mater. Sci. **6**, 15 (1996).
[7] W. Press, *Single-Particle Rotations in Molecular Crystals*, Springer Tracts Mod. Phys. (Springer Verlag, Berlin, 1981), Vol. 92.
[8] I. F. Silvera, Rev. Mod. Phys. **52**, 393 (1980).
[9] A. P. Smith *et al.*, Phys. Rev. B **53**, 10 187 (1996).
[10] L. Bengtsson *et al.*, Phys. Rev. B **61**, 16 921 (2000).
[11] B. Pajot *et al.*, Phys. Rev. B **62**, 10 165 (2000).
[12] W. Weltner and R. J. van Zee, Chem. Rev. **89**, 1713 (1989).
[13] Z. Li and J. S. Francisco, J. Chem. Phys. **96**, 878 (1992).
[14] S. Pellerin *et al.*, J. Phys. D **29**, 2850 (1996).
[15] Y. T. Shih *et al.*, Phys. Rev. B **54**, 10938 (1996).
[16] C. H. Wang, *Spectroscopy of Condensed Media* (Academic Press, Orlando, FL, 1985).
[17] The quantum gyroscope rotates at www.univie.ac.at/spectroscopy/QGy/QGyro.html